56 pi

EXPERIMENTAL STUDIES OF CHEMICAL NONEQUILIBRIUM IN HYDROGEN NOZZLE FLOWS

By: A.L. Russo, J.G. Hall, J.A. Lordi

Contract No. NASr-109
CAL Report No. AD-1689-A-4
June 1964

CORNELL AERONAUTICAL LABORATORY, INC.
OF CORNELL UNIVERSITY, BUFFALO 21, N. Y.

CORNELL AERONAUTICAL LABORATORY, INC.
BUFFALO, NEW YORK 14221

CAL REPORT NO. AD-1689-A-4

EXPERIMENTAL STUDIES OF CHEMICAL NONEQUILIBRIUM IN HYDROGEN NOZZLE FLOWS

JUNE 1964

CONTRACT NO. NASr-109

BY: A.L. Russo
A.L. Russo

J.G. Hall
J.G. Hall

J.A. Lordi
J.A. Lordi

APPROVED BY: A. Hertzberg
A. Hertzberg, Head
Aerodynamic Research Dept.

FOREWORD

The studies presented in this report were sponsored by the National Aeronautics and Space Administration under Contract NASr-109 as part of a general study of nonequilibrium gasdynamics related to propulsion systems.

Preliminary results from this study were previously reported in a paper presented at the American Physical Society Summer Meeting at the University of Washington, Seattle, August 1962. The abstract of this paper is contained in the Bulletin of the American Physical Society, Vol. 7, Paper F-4, 447. A summary of this work was presented at the AIAA Conference on Physics of Entry into Planetary Atmospheres held at Massachusetts Institute of Technology, Boston, Massachusetts, August 1963, (AIAA Paper 63-449).

26367

ABSTRACT

The effects of finite recombination rates on the flow of highly dissociated hydrogen in an argon bath have been studied in supersonic nozzle expansion flows of shock heated H_2/Ar mixtures. Nozzle-wall static pressure distributions have been obtained for expansions from a reservoir temperature of 6000°K and reservoir pressures of 28, 57 and 112 atm. The measured pressures show a definite departure from the values expected for equilibrium flow, and this is interpreted as due to lag in H-atom recombination during the flow expansion. Recombination rate constants were determined to about a factor of 2.5 by comparing the experimental pressure data with exact numerical calculations. The mean values of these recombination rate constants were found to be in agreement with corresponding rate constants deduced from shock-wave dissociation results.

author

TABLE OF CONTENTS

1. INTRODUCTION

In many of the high enthalpy gas flows of current aerophysical interest, the gas is characterized by high stagnation temperatures which can result in the excitation of the normally inert energy modes of vibration, dissociation, and ionization. This situation can prevail, for example, in the external flow about hypersonic vehicles[1-3] as well as in various internal flows such as those in high-performance rocket nozzles[4-6] and hypersonic wind-tunnels[7-9]. In the calculation of these flows, it is necessary to couple reaction rate equations with the usual gasdynamic equations[10] to account for the different rates of equilibration of vibration, dissociation, and ionization with the translational and rotational degrees of freedom. The lag in the equilibration of these normally-inert modes with the rotational and translational modes can reduce the kinetic energy of the gas flow. Furthermore, these nonequilibrium processes can significantly effect the radiative, transport, and electromagnetic properties of the gas (see e.g. Refs. 11, 12 and 13 respectively). A discussion of nonequilibrium in expansive flows is given in Ref. 14.

Machine computer programs have been developed at CAL which enable exact numerical solutions to the coupled relaxation and gasdynamic equations for both shock wave[15] and expansion-type[16] flows to be obtained providing the phenomenological description of the rate processes is known. However, the reaction rates required in the relaxation equations are often subject to large uncertainties. A great deal of effort has been expended in recent years to obtain appropriate high-temperature chemical rate data in flames (Ref. 17) and in shock wave flows (Refs. 18-21). These

experiments entail the study of flows in which molecular dissociation is the predominant process in the approach to the final equilibrium state attained. It is assumed that recombination-rate constants appropriate to expansion flows may be inferred from such shock-tube measurements on the basis that the equilibrium mass-action law is valid for nonequilibrium conditions. However, this assumption and the extrapolation of the shock-tube measured rates to nozzle flows where the thermo-gas-dynamic environment is very different may be open to question[31].

There is a need to verify the extrapolation of shock-wave chemical rate data to expansion flows and to obtain direct measurements of the recombination rate constants where possible. This is particularly evident as regards the use of hydrogen as a high-temperature rocket propellant. Theoretical estimates of hydrogen rocket performance show that small changes in the frozen atom concentration can result in significant changes in specific impulse.[6] The technical importance of the dissociation-recombination kinetics of hydrogen is evidenced by the recent research emphasis on dissociated H_2 flows[18-21]. While this interest in H_2 stems mainly from its potential as a rocket propellant, the kinetics involved also have a fundamental significance as regards the expansion of other dissociated gases, such as in the flow of air about re-entry bodies. Despite the emphasis on H_2 kinetics, it may be noted that hydrogen-atom recombination rates inferred by various investigators from shock wave dissociation studies (Refs. 18-21) vary by about an order of magnitude.

In the present nozzle-flow studies, the measurement of static pressure distributions in the nozzle were used to determine the departure

from equilibrium due to freezing of the hydrogen atom concentration. For this purpose a hydrogen-argon test gas mixture was shock heated and compressed in a shock tube[22] to an equilibrium reservoir temperature of 6000°K and reservoir pressures of 28, 57 and 112 atm. The gas in the reflected shock region then served as a reservoir for steady-flow expansion of millisecond duration in either of two supersonic nozzles coupled to the end of the shock tube.

When the relaxing energy mode contains a significant portion of the total energy of the expanding gas, large effects due to nonequilibrium in this mode on the pressure distribution may be anticipated. At the above reservoir conditions, the hydrogen was more than 90% dissociated in all cases, the energy in dissociation represented about 20% of the total enthalpy. Thus, a lag in hydrogen atom recombination was expected to result in sizable departures of the static pressure distributions from equilibrium. Further, because of the high level of dissociation and the high natural frequency of the H_2 vibration, the energy in molecular vibration in the reservoir was small so that departures from equilibrium could be reasonably attributed to a lag in atom recombination alone.

The purpose of the present experiments was two-fold: first, to determine the extent, if any, of the departure from chemical equilibrium of the expanding test gas by measuring the static pressure distributions along a nozzle wall; second, to interpret the observed pressure distributions in terms of hydrogen-atom recombination rates by comparing the experimental data with exact numerical solutions. The nozzle-wall static pressure measurements of dissociated H_2 + Argon expansions are discussed

in Sec. 3.1. These measurements were corrected for nozzle-wall boundary layer and compared with corresponding theoretical distributions calculated for equilibrium and frozen flows. These comparisons indicate that for the range of reservoir pressures used, the experimental pressures were generally below the limit for equilibrium hydrogen dissociation, but above the limit for frozen dissociation. This reduction in pressures below the corresponding equilibrium values is attributed to a lag in hydrogen atom recombination during flow expansion. The departure from equilibrium was found to increase with decreasing reservoir pressure in accordance with this interpretation.

The experimental data were used to infer recombination rates by comparison with exact numerical solutions for the finite-rate flows as described in Sec. 3.2. In the numerical calculations the recombination rates were varied both with respect to magnitude and temperature dependence. A single set of rate constants, independent of temperature, was determined to about a factor of 2.5 which gave reasonable agreement between theory and experiment.

2. EXPERIMENTAL TECHNIQUE

2.1 Apparatus

Shock Tube

The shock tube used for the present studies consisted of a high pressure driver and a low-pressure driven tube separated by a metal diaphragm. The downstream end of the driven or test gas tube is coupled to a convergent-divergent supersonic nozzle. The upstream portions of the nozzles (both wedge and conical type) are contoured and rapidly become plane and normal to the tube axis to provide almost complete reflection of the incident shock wave. The driver is 12 ft. long, 3-1/2 in. I.D. and is capable of operation at pressures up to 30,000 psi. Helium and hydrogen were both used as driver gases in this work. The driven tube is 20 ft. long with a square internal cross-section 2-1/2 x 2-1/2 in. and has a maximum allowable pressure of 5000 psi.

The downstream half of the shock tube is instrumented at a number of locations with thin-film resistance thermometers which are used as time-of-arrival gages for the incident shock wave. The incident wave speed was determined by recording the passage of the shock wave over the thin-film gages on an oscilloscope trace with calibrated 10 μsec markers superimposed. This system enables the wave speed to be determined to within 1%. In addition, the last station in the driven tube, about 3-5/8 in. from the nozzle entrance (reflecting wall), is instrumented for pressure measurement and also contains small viewing windows for spectroscopic (line-reversal) measurements. Initial test-gas pressures were monitored on a bank of four Wallace and Tiernan precision dial-manometers with

overlapping ranges covering the pressure range 0-800 mm Hg abs. The driven tube was evacuated prior to each run to less than 0.2 microns of Hg abs and had an apparent rate of pressure rise of about 1 micron per minute at this vacuum level.

Supersonic Nozzles

Two supersonic nozzles were used in the present studies; a 15° two-dimensional convergent-divergent wedge-type nozzle and a 15° convergent-divergent conical nozzle. Either nozzle couples to the end of the shock tube and discharges into a large tank. The contours of both nozzles are smooth to the extent that their second derivatives are continuous throughout.

The wedge nozzle is 2-1/2 inches wide to match the 2-1/2 x 2-1/2 inch cross-section of the shock tube. Seven instrumentation ports are located in each of the parallel nozzle walls. The first instrumentation port is located at the nozzle throat. These ports can accomodate pressure transducers, thin-film heat transfer gages or small windows for optical studies. At the most downstream station, 6 inch diameter windows can be mounted for schlieren studies of model flow fields, and to permit optical determination of the local boundary layer thickness on the contoured nozzle walls.

This wedge nozzle was used in preliminary work to develop the shock mountings for the pressure instrumentation, to optimize the orifice-cavity arrangement of the pressure transducer mountings with respect to rise time and spatial resolution, and to study the nature and extent of wall boundary layer. The shock mounting technique will be discussed below and the calibration studies are discussed in the appendix.

The conical nozzle Fig. 1 has a 3/8-inch diameter throat, upstream of which the contour becomes plane normal to the tube axis. A few inches downstream of the throat the contour becomes conical with a total included angle of 15°. Incorporated in the walls of this nozzle is the orifice arrangement and shock mounts developed in the wedge nozzle. The conical nozzle wall was instrumented for static pressure measurement in this manner at area ratios of $A/A^* = 4, 8, 16, 32, 64$ and 128. More recently, additional provision has been made to permit simultaneous heat transfer and optical (spectroscopic) measurements. This nozzle was used for the non-equilibrium flow studies because its more rapid expansion rate is conducive to earlier departures from equilibrium, and its mass flow rate is small.

Prior to each experiment the nozzle and discharge tank were isolated from the shock tube by means of a scribed copper diaphragm located at the nozzle entrance. The nozzle-tank combination was then evacuated to less than 0.1μ Hg and had a total apparent rate of pressure rise of about 0.1μ Hg per minute. Following the bursting of the driver-driven diaphragm, the pressure rise behind the reflected shock wave at the end of the driven tube (at the nozzle entrance) was sufficient to burst the copper diaphragm but not fragment it. Thereupon, steady flow was established through the nozzle in a time of the order of a few hundred microseconds.

2.2 Pressure Measurement Technique

The measurement of static pressure distribution in the nozzle is used to determine the departure from equilibrium values due to freezing of atom concentration. The static pressure is a basic gasdynamic variable

whose measured distribution effectively defines and/or assesses the actual fluid dynamics of the flow being studied. Confirmation of the basic thermo-gas-dynamic environment is obviously necessary in order to employ with confidence more difficult or refined diagnostic techniques. Where the non-equilibrium process of interest involves sufficient enthalpy and the gas is sufficiently expanded, the measurement of static pressures can be a useful method (if not the only ready method) of detecting departures from equilibrium in flows of this type.

The present approach to the measurement of the static-pressure distribution in the flow has been to instrument the nozzle wall with flush mounted transducers rather than attempt to develop static pressure probes for insertion into the flow as done by some workers (e.g. Ref. 23). Notwithstanding the more serious mechanical-shock isolation problem encountered, wall mounted transducers were used because essentially no problem whatsoever is presented as regards basic interpretation.

In the present experiments, Kistler piezoelectric quartz crystal transducers, model 401 (PZ14) were used to measure nozzle-wall static pressures. This transducer has a sensitivity of 4μμcb/psi over the range of pressures calibrated, namely 0.1 to 3000 psi, with a natural frequency of 50KC. The direct calibration of the transducer is by a dead-weight tester over the range 30 to 3000 psia. Below 30 psia, a simple dynamic calibration method was used which entails exposing the transducer to a large reservoir of gas at a known pressure by means of a rapid-acting mechanical valve. The calibrations are linear over the above pressure range and reproducible to within 2% even after several months usage. As with any very

high-impendance transducer, it is necessary to take particular precautions to avoid charge leakage due to dirt or moisture in order to obtain consistent performance.

Transducer response to acceleration of the nozzle wall occurring mechanically was minimized by the use of a relatively massive and soft vibration mount having a low natural frequency. The natural frequency of the nozzle wall itself was made relatively high for the conical nozzle by appropriate structural design. The salient features of the shock mounts used in the wedge and conical nozzle are shown in Fig. 2. The transducer is imbedded in a brass block which contacts the nozzle wall only through soft "O" rings. The stiffness of the mounting was varied by mechanical compression. The acceleration response of the transducer and shock mount was evaluated (in the wedge nozzle) by shielding the transducer from the flow and recording the output of the transducer for sensitivity levels comparable to those anticipated for the actual pressure measurements. The optimum combination of "O" ring hardness and compression were then used in the conical nozzle. To obtain good spatial resolution and provide a combined heat sink and shield to minimize temperature effects, the transducer diaphragm is located a few thousandths of an inch behind an orifice disc flush with the nozzle wall. The orifice disc is integral with the wall for the conical nozzle (see Fig. 2). Orifice diameters range from about 1/16 to 1/8 inch, depending on the nozzle area ratio of the pressure station, and the orifice depth (i.e., local wall thickness in the case of the conical nozzle) is about 1/32 inch. Adjustment of the orifice-cavity geometry was made until the response time of the system at any station

was within the nozzle flow starting time. That is, further increase in orifice did not reduce the time for the transducer to record a constant pressure level.

In general, the performance of this transducer system has proved satisfactory. The lower limit of measureable pressure is currently about 1/4 psi. This limit could probably be reduced further by additional improvement of the mechanical isolation.

2.3 Nozzle-Wall Boundary Layer Calibration Studies

For the nozzle flows, the boundary layer generally exerts a relatively small effect on static pressure. Nevertheless, it can have a very large effect on rate constants inferred from pressure measurements because of the relative insensitivity of the static pressure to flow chemistry. In order to interpret the data from the present experiments with some confidence, extensive flow calibration studies were conducted to assess the nature and the extent of the boundary layer on the nozzle walls. In these studies static pressure distributions were obtained for nozzle flows of helium, nitrogen and argon in which negligible real gas effects were present. The reservoir conditions included a range of pressures and temperatures (to provide adiabatic as well as highly cooled wall conditions) and covered the range of Reynolds numbers (5×10^5 to 2×10^7) anticipated for the hydrogen relaxation studies. Good agreement was obtained between the experimental data and the pressure distributions calculated from one-dimensional theory when the latter were corrected for the effect of displacement thickness by semi-empirical formulas for turbulent boundary layer. The existence of turbulent boundary layer was substantiated by heat transfer measurements

at the nozzle wall. The typical agreement between the experimental and theoretical results is illustrated in Fig. 11 and a detailed description of these calibration studies is contained in the appendix.

3. HYDROGEN RECOMBINATION STUDIES

Large effects on the gasdynamic variables due to nonequilibrium in an expansion flow can be obtained when the relaxing mode contains a significant portion of the total energy of the test gas.[30] In order for large amounts of chemical energy to be made unavailable due to freezing of the hydrogen atom concentration during expansion, it is necessary to have a large degree of dissociation in the reservoir prior to the expansion. A detailed study of the reservoir conditions attainable for hydrogen-argon mixtures was carried out by means of a machine computer program. Numerical solutions for thermochemical equilibrium for both incident and reflected shock waves were obtained for a range of H_2-Ar mixtures and for various initial pressures.

Approximate solutions were obtained on the basis of these results for finite-rate flows in the nozzle using the relaxation-length method previously developed in Ref. 8. Estimates were obtained of the departure from equilibrium of the static pressure which would occur for a range of nozzle area ratios. The results indicated that the use of an 8% H_2 + 92% Ar test gas mixture could result in reductions of the equilibrium static pressure distributions in the nozzle by about 30% due to nonequilibrium. This test gas mixture would also permit the use of initial shock tube pressures in the range of about 0.1 to 1 atm which would correspond to reservoir pressures of about 30 to 300 atm. at stagnation temperature of about 6000°K. Under these high pressure conditions, thermochemical equilibrium behind the reflected shock would also be attained.

A premixed cylinder of H_2-Ar test gas for the nonequilibrium studies

was obtained from The Matheson Company, Inc. of East Rutherford, New Jersey. The laboratory report of the gas analysis, furnished by the supplier, indicated the following composition:

H_2	7.95%
Hydrocarbons	less than 100 PPM
N_2	less than 100 PPM
Argon	balance

In Section 3.1 the experimental static pressure measurements will be discussed and the method for obtaining recombination rates by comparisons of the experimental data with exact numerical solutions for the flow will be described in Section 3.2.

3.1 Experimental Data

The initial experiments were carried out in the conical nozzle at equilibrium reservoir conditions of 6000°K and 57 atm pressure. These conditions were determined from the measured speed of the incident shock wave and the initial test gas conditions. In each experiment the reservoir pressure was measured with the PZ14 transducer and the shock tube wall-temperature history near the nozzle entrance was monitored by a thin-film resistance thermometer. The wall temperature history was found to provide a good indication of the uniformity of reservoir conditions, including the effects of temperature, pressure and gas composition.

A threefold criterion was used to determine which experiments warranted detailed analysis. First, the measured reflected shock pressure must agree to within the reliability of the transducer (about $\pm 5\%$) with the

pressure calculated on the basis of the measured wave speed. For suitable agreement, the equilibrium reservoir conditions were taken to be those calculated from the measured wave speed. Second, the test flow duration as indicated by the wall temperature history at the nozzle inlet must be longer than the combined nozzle starting time* and the rise time of the pressure instrumentation. Third, the nozzle wall static pressures must attain a constant value within the test flow duration.

The range of free stream Reynolds numbers in these experiments was 0.5×10^6 to 2×10^6 based on axial distance from the nozzle throat. The geometric area ratios at which the measurements were made were corrected for turbulent boundary layer by reducing the local diameter by the displacement thickness calculated from Eq. (1) of the appendix. The local displacement thickness was calculated to be less than 10% of the nozzle diameter. On the basis of inviscid-flow calculations for finite reaction rates, the effect of nonequilibrium on the calculated displacement thickness was found to be negligible.

A typical pressure record taken in the nozzle which clearly illustrates the salient features of the nonequilibrium flow is shown in Fig. 3. The oscilloscope sweep is initiated before rupture of the nozzle diaphragm to establish the no-flow reference level of about 600 μsec duration. The acceleration sensitivity of the transducer and mount is noted by the slight low frequency noise signal which persists throughout the record. The flow starting processes result in a marked and rapid increase in nozzle pressure.

*That is, the time lapse after rupture of the nozzle diaphragm which is necessary to establish steady flow conditions in the nozzle.

The starting process requires about 400 μsec, after which time a steady static pressure level persists for about 600 μsec. A second rise in pressure terminates the useful flow. This second increase in static pressure is due, in part, to changes in the effective specific heat ratio for the expansion from the test gas ($\gamma \cong 1.6$) to the Hydrogen driver gas ($\gamma = 1.4$) together with thickening of the boundary layer due to rapid decrease in stagnation temperature. With increasing reservoir pressure, the pressure differential between the first (test gas) and the second pressure levels decreases because of the smaller departures of the test gas from equilibrium as a direct result of higher reservoir pressure.

Typical measured pressure distribution obtained from the initial experiments at 57 atm reservoir pressure are compared in Fig. 4 with the calculated limits for chemically frozen and equilibrium inviscid (source) flow. The geometric nozzle area ratios at which the pressure data were obtained have been corrected, as described, to account for wall boundary layer. The measured static pressures shown in Fig. 4 are seen to lie below the limit for equilibrium chemistry but above that for completely frozen flow chemistry and these limits differ by a factor of two. In this case the corrections to the geometric area ratios to account for boundary layer are rather small, and the experimental data indicate lower than equilibrium pressures even without such corrections. The maximum scatter in the data occurs at the lowest pressure level and is somewhat less than $\pm 10\%$ of the corresponding mean value. The reduction in observed pressure from the calculated equilibrium limit is considered to be a real effect, not in doubt on account of either data scatter or boundary layer effect. This pressure reduction is interpreted as

evidence of a lag in hydrogen-atom recombination occurring in the flow expansion process.

Additional pressure measurements were made for reservoir pressures of 28 and 112 atm at the same reservoir temperature of 6000°K. A plot of all the measured pressure data, corrected for boundary layer, is shown in Fig. 5 along with the calculated limits for equilibrium and frozen flow for 57 atm. It is noted that these calculated limiting curves are essentially independent of reservoir pressure over the range covered.

The measured pressure data of Fig. 5 show greater reduction from the equilibrium limit with decreased reservoir pressure. This trend is to be expected on the basis of (lagging) recombination of hydrogen atoms occurring via three-body collisions. Three-body recombination has an order greater dependence on pressure (density) than has a two-body collision process such as dissociation. The experimental data of Fig. 5 for the lowest reservoir pressure of 28 atm are seen to lie close to the calculated frozen limit, while those for the highest reservoir pressure of 112 atm lie close to the equilibrium limit.

While the general trend of the pressure data in Fig. 5 is thus clear, two detailed features which are not understood should be noted. First, at the highest measured pressures where the corrected area ratio is slightly less than 4 the data cluster together for all reservoir pressures, rather than showing the separation present elsewhere. Second, at the highest reservoir pressure of 112 atm, the experimental data at the two largest area ratios tend to lie slightly higher than the calculated equilibrium limit. These two features have been found to be quite reproducible. Although a satisfactory explanation of their occurrence is not readily apparent, it is not considered

that either of the effects influence the general interpretation of the data in terms of a lag in recombination. However, because of the anomolies the data for a reservoir pressure of 112 atm were not used for the purpose of inferring recombination rates as described below.

3.2 Inferred Recombination Rates

The experimental data for 28 atm and 57 atm reservoir pressures were considered sufficiently accurate to warrant comparison with calculated pressure distributions for the purpose of inferring recombination rate constants. Calculations of the inviscid expansion flow for finite reaction rates and the particular geometry of the 15° conical nozzle were carried out numerically using an existing IBM machine code previously developed at CAL (Ref. 16). Within the framework of the assumed kinetic processes, and for pseudo-one-dimensional (or source) flow without transport phenomena, this code provides an exact numerical solution to the nonequilibrium flow. The initial conditions for starting the calculations were taken to be the equilibrium conditions in the reservoir. For the 57 atm reservoir pressure, equilibrium conditions were assumed to prevail up to the nozzle throat. The latter assumption was justified on the basis that exact solutions indicated little or no nonequilibrium at the nozzle throat for the higher reservoir pressures.

The reaction mechanism assumed in these calculations was the dissociation-recombination reaction

$$H_2 + X \underset{k_r}{\overset{k_d}{\rightleftharpoons}} H + H + X$$

where X represents any of the possible collision partners Ar, H, or H_2. In the computer program the forward and reverse rate constants, k_D and k_R, are assumed to be related by $\frac{k_D}{k_R} = K(T)$ where $K(T)$ is the local equilibrium constant which depends only on the translational temperature. Recombination rate constants obtained from shock-wave dissociation studies, shown in Fig. 6, were used as guides for assuming specific rate constants for the calculations. The approach in the present analyses was to try to find numerical solutions using various reaction rates which were consistent with the experimental observations. The specific reaction rates were varied both with respect to magnitude and temperature dependence with the assumption that the recombination rate is proportional to some power of the translational temperature i.e. $k_R = AT^n$.

In the first series of calculations, for the 57 atm reservoir pressure case, the values of k_R for each of the third body collision partners in the reaction mechanism were taken to be constant and independent of temperature. Values of k_R corresponding approximately to the smallest values inferred in the previous shock wave studies in H_2-Ar mixtures[18-21] shown in Fig. 6, were used to obtain the lower curve, I, shown in Fig. 7. This curve is seen to correspond approximately to the lower limit of the scatter of the experimental pressure data at 57 atm. The magnitudes of the recombination rates were then increased until the upper curve, II, of Fig. 7 was obtained. Curve II represents an increase in the rate constants by a factor of about six and corresponds to pressures about 10% higher than in Curve I.

It is noted that this factor of about six corresponds to the range of variation in recombination rates inferred from shock-wave dissociation

studies in H_2-Ar mixtures by various investigators. Further, the 10% difference in pressure between curves I and II also corresponds to the average scatter of the present pressure data.

The particular values of the rate constants employed in obtaining curves I and II are tabulated in Fig. 7. The dominant rate constant in these calculations is that for the hydrogen atom as the third body. This rate constant is sufficiently large that, despite the relatively low concentration of H as compared to Ar, the actual rate of atom recombination due to H as a third body exceeds that due to Ar as a third body. Thus, the difference in static pressure distributions between curves I and II is largely due to the corresponding change in k_ℓ for H as the third body. This difference in static pressure would not be strongly affected by changes of a different magnitude in k_ℓ for Ar and H_2 as third bodies. The hydrogen molecule, in particular, was noted from the calculations to be relatively unimportant as a third body because of its very low concentration.

The fact that a change of a factor of six in rate constants produces a change in the calculated pressures of only about 10% illustrates the insensitivity of pressure to the flow chemistry and the basic difficulty of inferring rate constants from the pressure data. Taking the average scatter of the experimental data to be $\pm$5%, the best estimate of recombination rates to be inferred from the data at 57 atm reservoir pressure shown in Fig. 7 are the geometric mean values of the rates shown for curves I and II. The uncertainty in these mean values is then a factor of about 2-1/2. It will be noted that these mean values are within the range of variation of reported shock wave results (Fig. 6), as mentioned above.

The difficulty of determining a unique recombination-rate constant from such pressure data is further illustrated by a second series of calculations carried out to assess the effect of a temperature dependence of k_R. Figure 8 shows the results for the calculated pressure distributions for the H_2-Ar mixture at a reservoir pressure of 57 atm. The lower curve is identical to curve I of Fig. 7. The upper curve was calculated assuming all k_R values to be proportional to T^{-1} and matching with the k_R values for the lower curve at the nozzle throat ($T \cong 4500°K$). The slight difference between these two curves indicates that theoretical pressure distributions calculated assuming rate constants inversely dependent on temperature to a small power could equally well be fitted to the experimental data of Fig. 4. As a result, the present studies, like the shock wave studies, do not permit an accurate determination of the dependence of the recombination rate constant on temperature.

As a check of the applicability of the inferred reaction rates to other reservoir conditions, the geometric-mean rates obtained from the 57-atm data were used to obtain theoretical estimates for the pressure distributions for the lower, 28 atm, reservoir pressure case. A comparison of the results of these calculations with the corresponding experimental data for P_o = 28 atm is shown in Fig. 9 together with the results for P_o = 57 atm. As can be seen from this figure, the theoretical and experimental results are in good agreement for the higher reservoir pressure and in fair agreement for the lower reservoir pressure on the basis of a single set of rate constants. The experimental data for P_o = 28 atm generally tend to indicate slightly lower static pressures than the corresponding theoretical

predictions. On this basis, it would appear that the reaction rates required to predict the low pressure data would be somewhat slower than those used to obtain Fig. 9. Decreasing the reaction rates would on the other hand influence the agreement for the 57 atm case. In view of the influence of other parameters in the experiments, such as possible impurities of a catalytic nature, as well as the basic insensitivity of the static pressure to chemical nonequilibrium, further refinements in the recombination rate constants inferred above would not appear warranted. The results of Fig. 9 are considered to support, within the context and limitations of the experiments, the applicability of shock tube rate data and the concept of local thermochemical equilibrium to expansion flows of the present type.

It is of interest to note in Fig. 9 that a reduction in reservoir pressure of a factor of about 2 results in a sizable reduction in the static pressure distribution. This large effect is interpreted as particularly due to freezing early in the nozzle. That is, in the vicinity of the nozzle throat, gradients in the flow are very large so that small changes in the location of the onset of freezing (due, for example, to changes in ρ_o) can exert a large influence on the frozen atom-concentration. In this connection, the numerical solutions for the 28 atm reservoir pressure indicate that the flow begins to appreciably depart from equilibrium upstream of the nozzle geometric throat.

From the comparisons of Fig. 9 together with the foregoing discussion, it is concluded that the recombination rate constants for hydrogen in hydrogen-argon expansion flows are inferred to be to within a factor of about 2.5:

$k_R = 1.7 \times 10^{14}$ (cc/mole)^{2}sec^{-1} for Argon third body

$k_R = 1.2 \times 10^{15}$ (cc/mole)^{2}sec^{-1} for H_2 third body

$k_R = 4.9 \times 10^{15}$ (cc/mole)^{2}sec^{-1} for H third body.

Finally, it is noted that the present results for hydrogen atom recombination rate constants are in contrast to results recently reported by Widawsky et al.[24] These authors also employed static pressure measurements to observe nonequilibrium effects in nozzle expansions of dissociated H_2. In their tests they used pure H_2 initially dissociated by electric discharge, and tested at reservoir pressures around 1 atm. The recombination-rate constants which they inferred from their measurements tend to average substantially higher than the average of corresponding shock-wave rate constants. Detailed comparisons of the present results with their results are difficult because of the different reservoir conditions and test-gas mixtures employed.

4. CONCLUDING REMARKS

The present experiments were undertaken to observe the effects of chemical nonequilibrium in simple expansion flows characterized by a single dominant rate process. It was thereby hoped that observed effects would be definitive and could be interpreted with confidence.

The effects of finite recombination rates of highly dissociated hydrogen in an inert argon bath on the nozzle-wall static-pressure distribution have been studied in a supersonic nozzle flow. In view of the relative insensitivity of the static pressure distribution to flow chemistry, extensive nozzle-flow calibration studies were conducted to obtain accurate estimates for boundary layer. The experimental data for the H_2-Ar flows, corrected for boundary layer, clearly indicate a decrease in static pressure distribution from equilibrium values which is interpreted as freezing of the hydrogen atom concentrations.

Recombination rate constants were determined to a factor of about 2.5, from comparisons of the experimental pressure data with exact numerical calculations. While the experimental data did not offer a clear indication of the temperature dependence of the recombination rates, they did suggest that the temperature dependence may be small. In fact, the results suggest that recombination rates independent of temperature and corresponding in magnitude to those obtained from shock wave data can be used for the calculation of hydrogen expansion flows.

The sensitivity of the static pressure distribution in a nozzle to the flow chemistry increases with expansion. That is, at larger area ratios the pressure difference between the equilibrium and the finite-rate flows increases. However, the measurement of static pressure itself becomes

increasingly difficult. As a result, it would seem that in order to obtain more accurate estimates of recombination rates, diagnostic techniques more sensitive to flow chemistry are required. Such techniques might monitor the gas composition directly or perhaps measure the gas temperature.

APPENDIX

FLOW CALIBRATION EXPERIMENTS

1. Reservoir State

One of the prime advantages of the shock tube for the generation of high temperature, high pressure flows is the relative ease with which the thermochemical state of the shocked gas can be determined from a measurement of the shock speed and initial conditions. A detailed knowledge of the reservoir (reflected shock) conditions is, of course, of paramount importance for nonequilibrium studies. As a result, measurements of the reservoir pressure attained behind reflected shock waves were made over a wide range of conditions with the PZ-14 pressure transducer. The purpose of these measurements was to determine the reliability with which the reservoir pressure could be measured with this transducer and to determine the agreement of the measured pressure with that calculated on the basis of the measured wave speed. Agreement of the measured pressure with that calculated from measured wave speed and shock tube theory permits an accurate determination of the complete reservoir state of the gas. It is noted however that the pressure of the test and driver gases are the same at the interface and that, pressure measurement alone cannot be used to distinguish between the gases. Other measurements such as heat transfer and, more particularly, spectroscopic measurements are necessary.

Pressure measurements were made for under-tailored, tailored, and over-tailored shock wave conditions using both hydrogen and helium driver gases. With off-tailored shock tube operation, the measurement of reflected

shock wave pressure becomes increasingly important due to additional wave systems which originate from the reflected shock-interface interaction and reflect backwards and forwards.

The pure acceleration response of the pressure transducer system was obtained by tests in which the transducer was shielded from the gas. Typical oscillograph records of the reflected shock pressure obtained for near-tailored and off-tailored interface conditions are shown in Fig. 10. In general, the measured reservoir pressures were found to agree to within about 5% with the calculated pressures immediately behind the reflected shock wave. Detailed calculations further indicated that the final equilibrium pressure as well as the time dependent nature of the reflected shock pressure was predictable from simple shock tube theory.

Verification of the calculated reservoir temperatures was obtained by temperature measurements using the spectrum-line reversal method behind reflected shock waves in N_2. (The details of the spectrum-line reversal method and the apparatus used for these measurements are given in Ref. 25 which is concerned with vibrational de-excitation studies of N_2 in the same shock tube-conical nozzle apparatus.) The measured temperatures, which were restricted to below 3000°K by the upper limit imposed by the background reversal source, were in agreement with equilibrium values calculated from shock tube theory on the basis of both the measured pressure and the measured wave speed. Such good agreement for these studies, lent considerable confidence to the determination of the reservoir temperatures for those cases in which the temperature itself could not be or was not measured.

The aforementioned line-reversal measurements were also used to

determine whether the opening of the nozzle diaphragm produced any significant effect on the reservoir temperature. These spectroscopic temperature measurements were made with normal nozzle diaphragm rupture and with the nozzle entrance blanked-off completely. No difference in the measured temperatures was observed.

2. Nozzle Flow Calibration

Pressure Measurement

Calibration experiments were conducted in both the wedge and conical nozzles to determine the reliability of the pressure measurement techniques and to establish the nature and extent of wall boundary layer. In order to eliminate real-gas effects and cover a wide range of flow conditions, static pressure distributions were measured for test gas flows of helium, nitrogen and argon for a wide range of reservoir conditions. For each test gas used in these flow calibration studies, the pressure data indicated a scatter within $\pm 5\%$ of the mean value of the pressure observed at each nozzle station. In addition, the data indicated monatonically decreasing pressures with increasing area ratio. The experimental pressures, however, were higher than the values calculated for pseudo-one-dimensional, inviscid flow. The difference between the measured and calculated pressure distributions was attributed to nozzle wall boundary layer.

For the conical nozzle, reservoir temperatures and pressures of 300°K and 15 atm, 2000°K and 60 atm, and 4000°K and 1200 atm, were used for nozzle flows of helium, nitrogen and argon respectively. For the helium-flow calibration studies (T_o = 300°K and P_o = 15 atm), relatively large

differences between the measured and inviscid pressure distributions were observed. These large differences were interpreted as due to a turbulent boundary layer which in this case was made relatively thick by the lack of boundary layer cooling as a result of adiabatic wall conditions, (i.e. $T_w \cong T_o$). For the argon-flow studies on the other hand, a highly cooled wall ($\frac{T_w}{T_o}$ = 0.075) coupled with high reservoir pressures resulted in small deviations of the observed pressures from the inviscid values. In total, the pressure data from these calibration experiments provided a good means for evaluating a theoretical correction to the nozzle area ratio to account for boundary-layer displacement thickness. For this purpose, the pressure distributions calculated from inviscid pseudo-one-dimensional (or source-flow) theory were corrected for boundary-layer displacement as described below, and compared with the experimental data. The assumption of source flow for the inviscid-flow model is a good approximation for the conical nozzle geometry.

For the range of Reynolds numbers ($\sim 5 \times 10^5$ to 2×10^7), involved in the calibration experiments the nozzle wall boundary layer was assumed to be turbulent. The existence of turbulent boundary layers for the H_2-Ar test gas mixture was verified directly in the wedge nozzle by the measurement of nozzle-wall heat-transfer rates using thin-film resistance thermometers. These results will be discussed below. The displacement thickness, δ^* , was calculated from a semi-empirical formula after Burke.[26] The particular expression used in the present work is

$$\frac{\delta^*}{x} = 0.104\left(1+\frac{\gamma-1}{2}M^2\right)\left(1+1.5\frac{T_w}{T_0}\right)\left(\frac{\gamma-1}{8}\right)^{\frac{1+\omega-m}{m}} \frac{(M^2)^{\frac{(1+\omega)}{m}}}{Re_x^{1/m}} \qquad (1)$$

where ω is the exponent in the viscosity law $\mu \sim T^{\omega}$, $m = 3$ (after Burke[26]), Re_x is the local stream Reynolds number based on x, M is the local Mach number, and x is the distance from the throat where δ^* is taken to be zero. It may be noted that, apart from the present calibration experiments, this expression has previously been tested with a variety of experimental data and shown to be applicable over a wide range of Mach numbers. For the highly dissociated hydrogen plus argon flows the term $\left(1+\frac{\gamma-1}{2}M^2\right)$ in Eq. (1) was replaced by $\frac{T_0}{T_e}$ where T_e is the local free stream temperature obtainable from the exact numerical solutions. The specific heat ratio and value of ω were taken to be those for pure argon. The remaining parameters ρ, u and M were obtained from the computer solutions for each particular set of reaction rates.

Over the entire range of calibration experiments, agreement to within a few percent was generally obtained between the measured pressure distributions and those calculated by applying the above displacement thickness to reduce the inviscid flow area ratios. In order to illustrate typical results, calibration data for the nitrogen experiments are shown in Fig. 11. A typical oscilloscope record of the transducer response is shown in the upper right corner of this figure. The horizontal separation of the two theoretical curves indicates the effect of the wall boundary layer on the nozzle area ratio. The two sets of experimental pressure data indicate the

typical agreement with the corrected inviscid-theory, as well as the reliability of the pressure instrumentation. Similar agreement obtained in all calibration experiments permitted a confident assessment of boundary layer in the nonequilibrium flow experiments.

Heat Transfer Measurement

Some preliminary nozzle-flow studies using the hydrogen-argon test gas mixture were carried out in the 15° two-dimensional wedge nozzle for reflected shock gas temperatures in the range of 5000 to 6000°K and for stagnation pressures of about 20-100 atm. In these experiments the nozzle throat heigth was about 0.120 inches. Heat transfer rates to the nozzle wall were measured at two area ratios, $A/A^* = 6$ and $A/A^* = 16.5$, as well as the complete static pressure distribution along the opposite plane nozzle wall. In obtaining the heat transfer rates, the outputs of the thin film resistance thermometers[27] were integrated directly by an analog network.[28] A pulse method was employed for determining the thermal properties of the backing material.[29]

Static pressure measurements in the wedge nozzle indicated that the dissociated hydrogen-argon test gas mixture remained in near-equilibrium over a large portion of the expansion. At large area ratios, some departure of the measured pressures from equilibrium was noted. As would be expected, the effect of decreasing the stagnation pressure was to move the point of departure in the nozzle further upstream, corresponding to an earlier departure from equilibrium. The fact that the test gas flow remains in near-equilibrium over a large portion of the expansion was attributable to the reduced rate of expansion of the wedge nozzle.

The heat transfer rates to the nozzle wall for these flow conditions

were large, and indicative of turbulent wall boundary-layer conditions. The measured heat transfer rates were compared with those calculated using an equivalent flat-plate method. Together with the reference temperature concept for relating the compressible and incompressible skin-friction coefficients.[26] The particular equation used was

$$\dot{q} = \frac{0.029}{P_r^{2/3}} \rho_e u_e (h_o - h_w) \left(\frac{\rho_r}{\rho_e}\right)^{0.8} \left(\frac{\mu_r}{\mu_e}\right)^{0.2} \frac{1}{Re_x^{0.2}} \qquad (2)$$

where

P_r = Prandtl number

h = enthalpy

and subscripts o, r, e and w refer to stagnation, reference, free stream and wall conditions respectively. The reference temperature is obtained from

$$T_r = 0.22(T_o - T_w) + 0.5(T_w + T_e)$$

In calculating heat-transfer rates from Eq. (2), it was assumed that the H_2-Ar test gas flow remained in thermochemical equilibrium. The gas-dynamic variables required in this equation were obtained from machine solutions for the equilibrium flows and were taken to be those at the appropriate geometric area ratios. The Prandtl number and the viscosity were taken to be those for pure argon at the appropriate temperatures. Using this formulation, nozzle heat transfer rates were calculated for reservoir temperatures of 5000, 5500 and 6000°K corresponding to the range of experimental temperatures and for a stagnation pressure of 100 atm.

The experimental data were corrected to a common reservoir

temperature of 5500°K. The heat transfer rate over this limited range of stagnation temperatures was assumed to be proportional to some power of the stagnation temperature for a constant reservoir pressure. The particular power dependence was determined from a fit to the results calculated from Eq. (2) for real gas equilibrium flow for reservoir temperatures of 5000, 5500 and 6000°K. This power dependence was then used to scale the experimental data to a common reservoir temperature of 5500°K. The dependence of the heat transfer rates on reservoir pressure was taken to be given by Eq. (2), viz.

$$\dot{q} \sim p_o^{0.8}$$

The experimental heat transfer data for the two area ratios were normalized by $p_o^{0.8}$ and scaled to 5500°K reservoir temperature. These results are compared in Fig. 12 with the rates calculated from Eq. (2) with the assumptions noted earlier. The vertical bar corresponds to the scatter in the normalized heat transfer rates and the horizontal bar corresponds to the possible error in the actual area ratio due to boundary layer. This range of area ratios reflects the variations in the actual boundary layer thickness for the range of stagnation pressures. These data appear to be in fair agreement with, though somewhat lower than, the results obtained from Eq. (2) for turbulent boundary layer. The individual heat transfer rates for these two area ratios are shown as a function of reservoir pressure in Fig. 13. These data have again been scaled to a common reservoir temperature of 5500°K. The theoretical curves for 5500° reservoir temperature illustrate the 0.8 power dependence on the reservoir pressure. The experimental data, particularly at the smaller area ratio, also indicate the 0.8 power

dependence. The measured heat transfer rates appear to be about 20% lower than the theoretical values. In this connection it is noted that some measurements made in the flow of nitrogen at 2100°K reservoir temperature and 55 atm reservoir pressure indicated turbulent heat transfer rates about 10% lower than the corresponding theoretical values. The present data for H_2-Ar test gas mixture at reservoir conditions of 6000°K and 20-100 atm support the assumption of turbulent wall boundary layer.

REFERENCES

1. Hall, J. G., Eschenroeder, A. Q. and Marrone, P. V., Inviscid Hypersonic Airflows With Coupled Nonequilibrium Processes. CAL Rept. No. AF-1413-A-2, May 1962.

2. Vaglio-Laurin, R. and Bloom, M. H., Chemical Effects in External Hypersonic Flows. Hypersonic Flow Research, Vol. 7, pp. 205-254, Progress in Astronautics and Rocketry, Academic Press, 1962.

3. Lick, W., Inviscid Flow Around a Blunt Body of a Reacting Mixture of Gases. Rensselaer Polytechnic Institute, TR AE 5810, May 1958 and TR AE 5814, December 1958.

4. Kreiger, F. J., Chemical Kinetics and Rocket Nozzle Design. ARS Journal, Vol. 21, No. 6, November 1951, pp. 179-185.

5. Welde, K. A., Effect of Radical Recombination Kinetics on Specific Impulse of High Temperature Systems. Jet Propulsion, Vol. 28, No. 2, February 1958, pp. 119-120.

6. Hall, J. G., Eschenroeder, A. Q. and Klein, J. J., Chemical Nonequilibrium Effects on Hydrogen Rocket Impulse at Low Pressures. CAL Rept. No. AD-1118-A-8, November 1959.

7. Bray, K. N. C., Departure From Dissociation Equilibrium in a Hypersonic Nozzle. ARC 19, 983, March 1958.

8. Hall, J. G. and Russo, A. L., Studies of Chemical Nonequilibrium in Hypersonic Nozzle Flows. Proceedings of 1st Conference on Kinetics, Equilibria, and Performance of High Temperature Systems, Butterworths, London, 1960; Also CAL Rept. No. AD-1118-A-6, November 1959.

9. Boyer, D. W., Eschenroeder, A. Q. and Russo, A. L., Approximate Solutions for Nonequilibrium Airflow in Hypersonic Nozzles. CAL Rept. No. AD-1345-W-3, August 1960.

10. Emanuel, G. and Vincenti, W. G., Method for Calculation of the One-Dimensional Nonequilibrium Flow of a General Gas Mixture Through a Hypersonic Nozzle. AEDC-TDR-62-131, June 1962.

11. Allen, R. A., Keck, J. C. and Camm, J. C., Nonequilibrium Radiation From Shock Heated Nitrogen and a Determination of the Recombination Rate. AVCO RR 110, July 1961.

12. Moore, F. K., On the Viscosity of Dissociated Air. CAL Rept. No. RM-1396-A-2, September 1961.

13. Eschenroeder, A. Q. and Daiber, J. W., Ionization Nonequilibrium in Expanding Flows. CAL Rept. No. AF-1441-A-2, September 1960.

14. Bray, K. N. C., Chemical Reactions in Supersonic Nozzle Flows. Paper presented at Ninth Symposium (International) on Combustion at Cornell University, Ithaca, New York, August 27-September 1, 1962.

15. Marrone, P. V., Inviscid Nonequilibrium Flow Behind Bow and Normal Shock Waves, Part I. General Analysis and Numerical Examples. CAL Rept. No. QM-1626-A-12 (I), May 1963.

16. Eschenroeder, A. Q., Boyer, D. W. and Hall, J. G., Nonequilibrium Expansions of Air With Coupled Chemical Reactions. Phys. Fluids, Vol. 5, No. 5, May 1962, pp. 615-624.

17. Bulewicz, E. M. and Sugden, T. M., Transactions of the Faraday Soc. Vol. 54, p. 1855 (1958).

18. Gardiner, W. C., Jr. and Kistiakowsky, G. B., Thermal Dissociation Rate of Hydrogen. J. Chem. Phys., Vol. 35, No. 5, 1961, p. 1765.

19. Rink, J. P., Shock Tube Determination of Dissociation Rates of Hydrogen. J. Chem. Phys., Vol. 36, No. 1, 1962, p. 262.

20. Patch, R. W., Shock Tube Measurement of Dissociation Rates of Hydrogen. J. Chem. Phys., Vol. 36, No. 7, 1962, p. 1919.

21. Sutton, E., Measurement of Dissociation Rates of Hydrogen and Deuterium. J. Chem. Phys., Vol. 36, No. 11, 1962, p. 2923.

22. Hertzberg, A., Wittliff, C. E. and Hall, J. G., Summary of Shock Tunnel Development and Application to Hypersonic Research. CAL Rept. No. AD-1052-A-12, July 1961; Also, Hypersonic Flow Research, edited by F. R. Riddell, Academic Press, New York, 1962.

23. Nagamatsu, H. T., Workman, J. B. and Sheer, R. E., Jr., Hypersonic Nozzle Expansions of Air With Atom Recombination Present. Journal of Aerospace Science, Vol. 28, No. 11, 1961, p. 833.

24. Widawsky, A., Oswalt, L. R. and Hays, J. L., Jr., Experimental Determination of the Hydrogen Recombination Constant. ARS Journal, Vol. 32, No. 12, December 1962, p. 1927.

25. Hurle, I. R., Russo, A. L. and Hall, J. Gordon, Spectroscopic Studies of Vibrational Nonequilibrium in Supersonic Nozzle Flows. J. Chem. Phys., Vol. 40, No. 8, 1964, p. 2076.

26. Burke, A. F., Turbulent Boundary Layers on Highly Cooled Surfaces at High Mach Numbers. CAL Rept. No. 118, November 1961.

27. Vidal, R. J., Transient Surface Temperature Measurements. CAL Rept. No. 114, March 1962.

28. Skinner, G. T., Analog Network to Convert Surface Temperature to Heat Flux. CAL Rept. No. 100, February 1960; Also, ARS Journal, Vol. 30, No. 6, June 1960, pp. 569-570.

29. Skinner, G. T., A New Method for Calibrating Thin Film Gauge Backing Materials. CAL Rept. No. 105.

30. Eschenroeder, A. Q., Boyer, D. W. and Hall, J. G., Exact Solutions for Nonequilibrium Expansions of Air With Coupled Chemical Reactions. CAL Rept. No. AF-1413-A-1, May 1961.

31. Bauer, S. H., Chemical Kinetics: A General Introduction. Hypersonic Flow Research, Vol. 7, pp. 143-180, Progress in Astronautics and Rocketry, Academic Press, 1962.

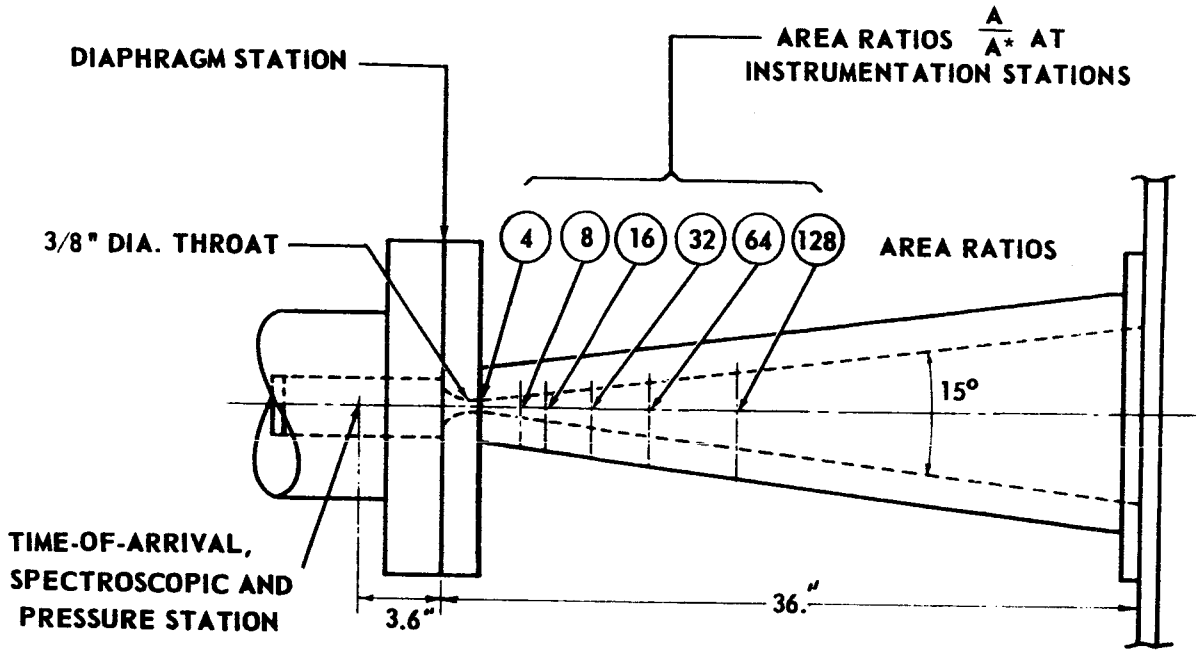

15° CONICAL NOZZLE

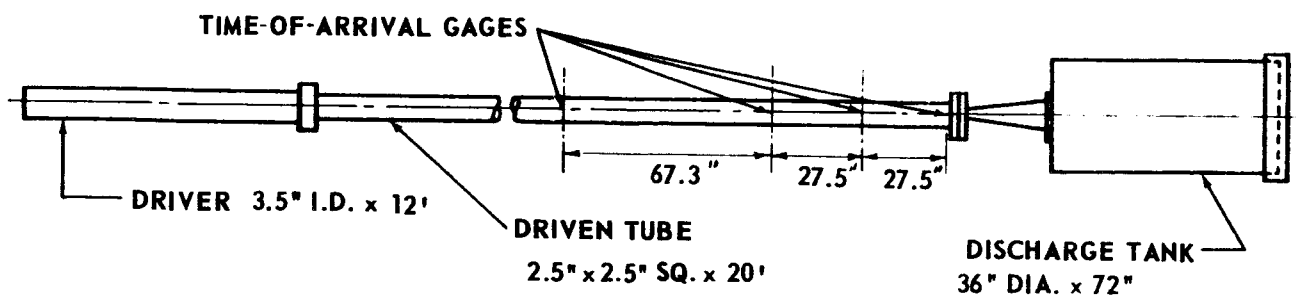

Figure 1 SHOCK TUBE-NOZZLE-DISCHARGE TANK ASSEMBLY

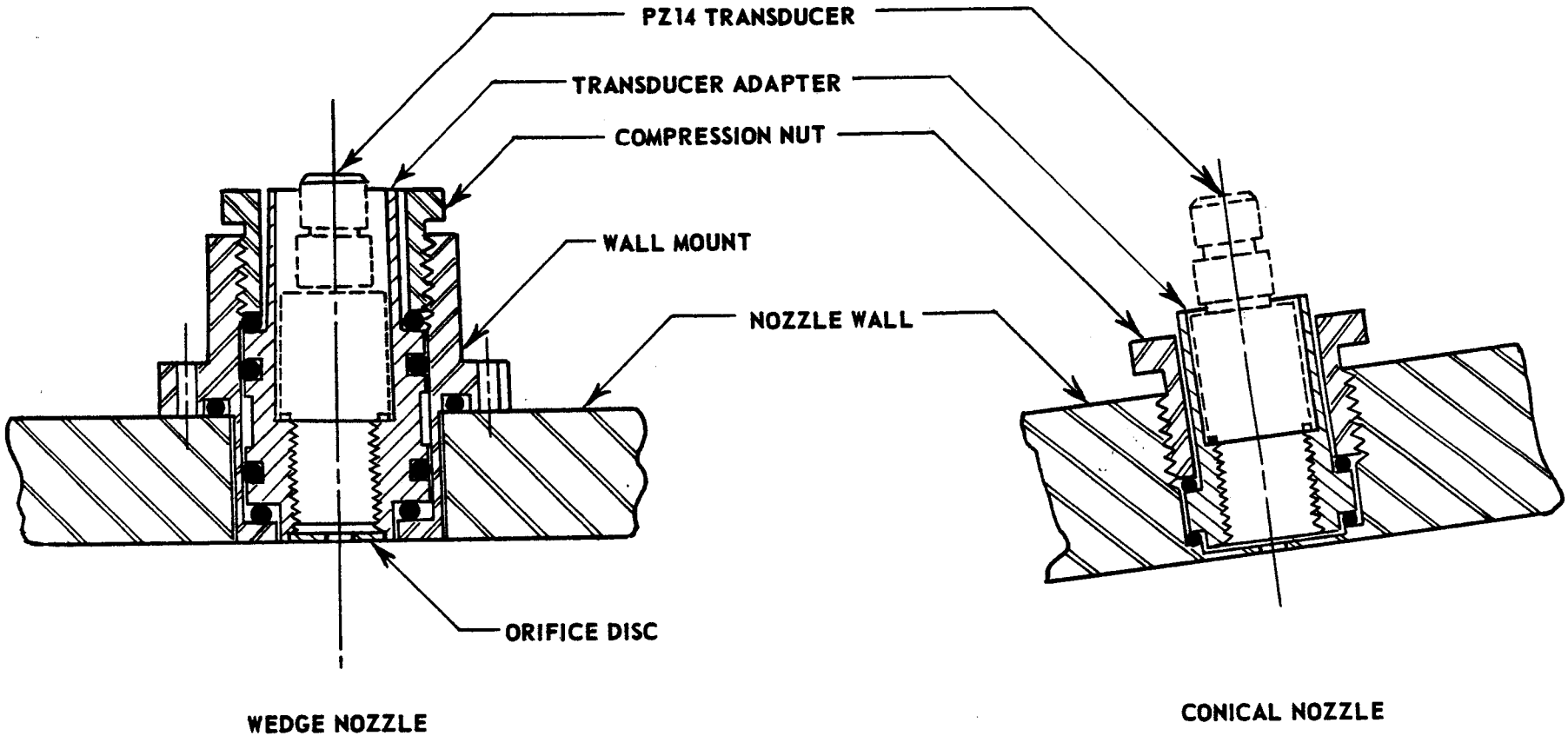

Figure 2 SCHEMATIC OF PRESSURE TRANSDUCER SHOCK MOUNTINGS USED FOR THE 15° WEDGE AND CONICAL NOZZLES

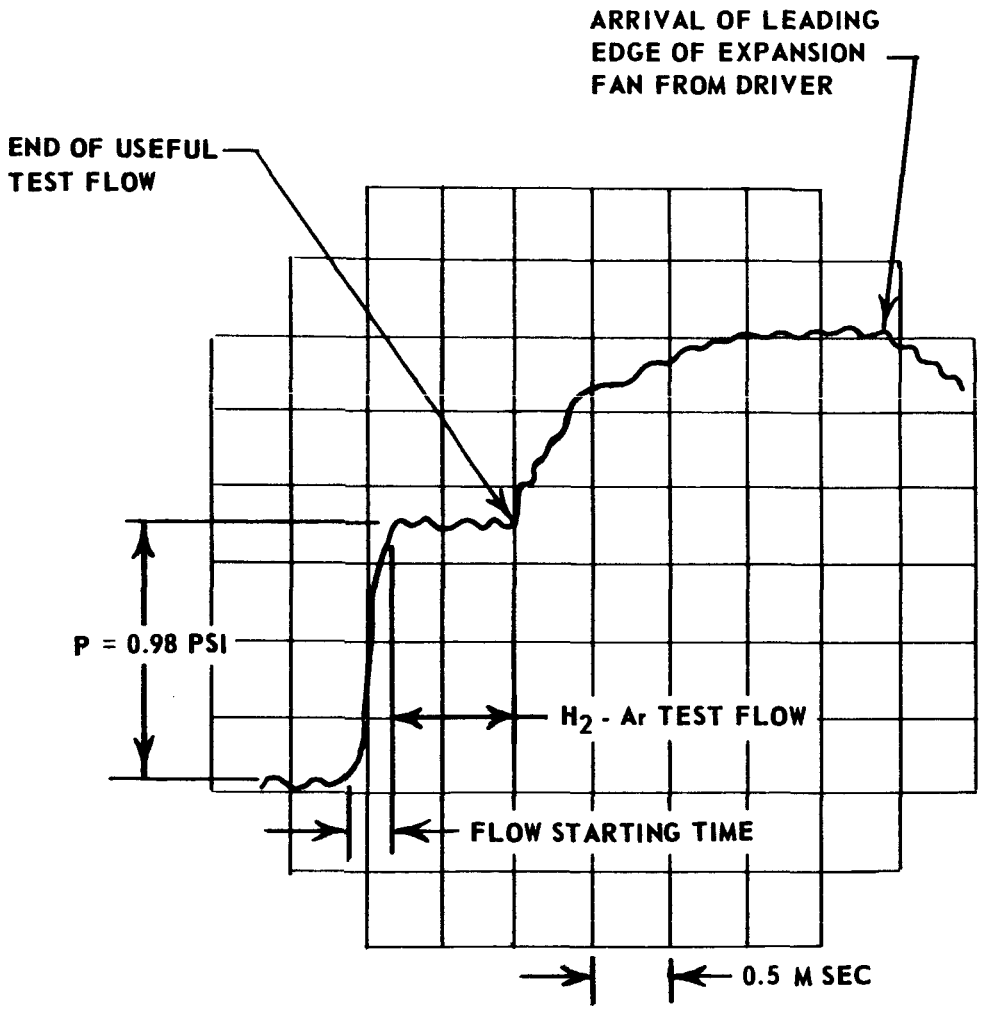

Figure 3 TYPICAL OSCILLOGRAPH RECORD OF STATIC PRESSURE OBTAINED IN THE CONICAL NOZZLE AT A/A^* = 16 FOR FLOW OF 7.95% H_2 + 92.05% Ar. T_o = 6000°K, P_o = 28 ATM

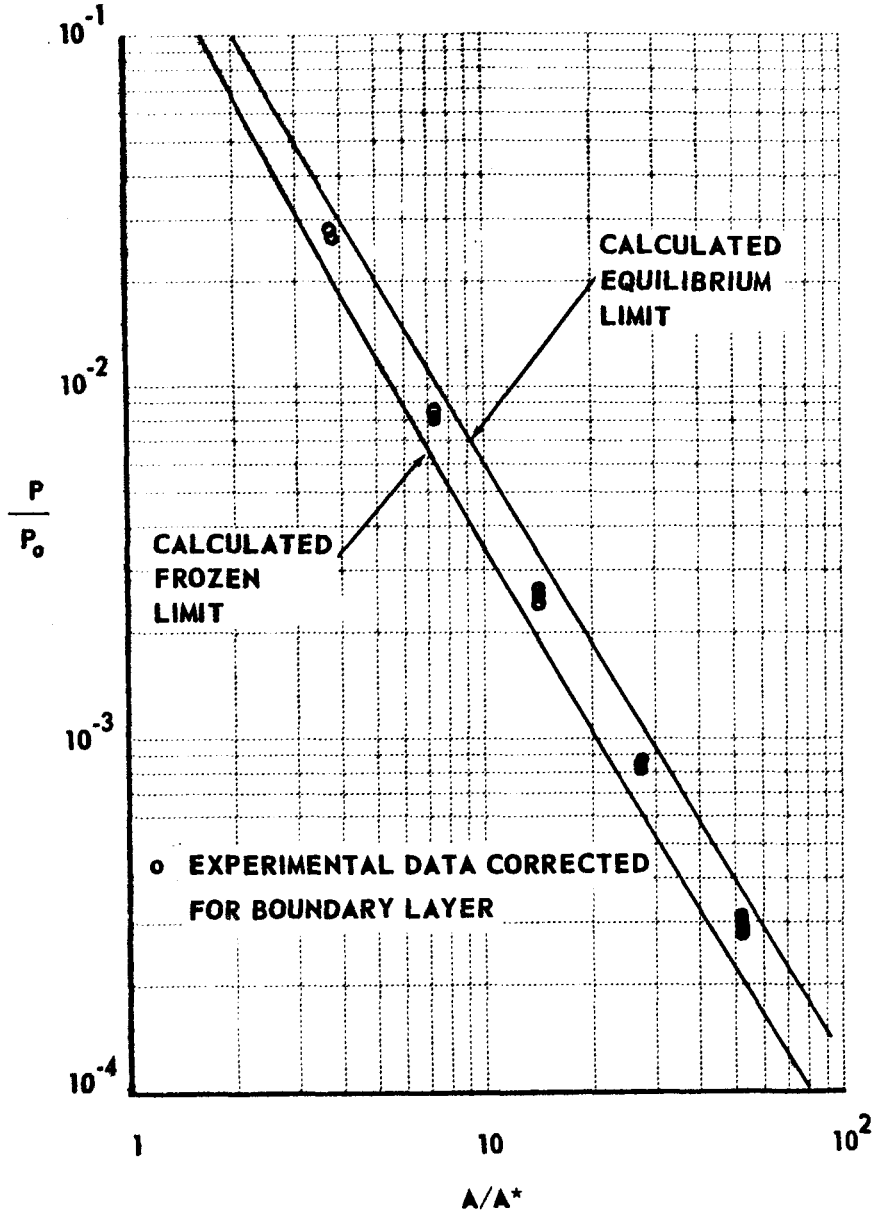

Figure 4 MEASURED PRESSURE DISTRIBUTION FOR FLOW OF DISSOCIATED H_2-Ar MIXTURE IN 15° CONICAL NOZZLE. T_o = 6000 °K, P_o = 57 ATM UNDISSOCIATED MIXTURE 7.95% H_2 + 92.05% Ar

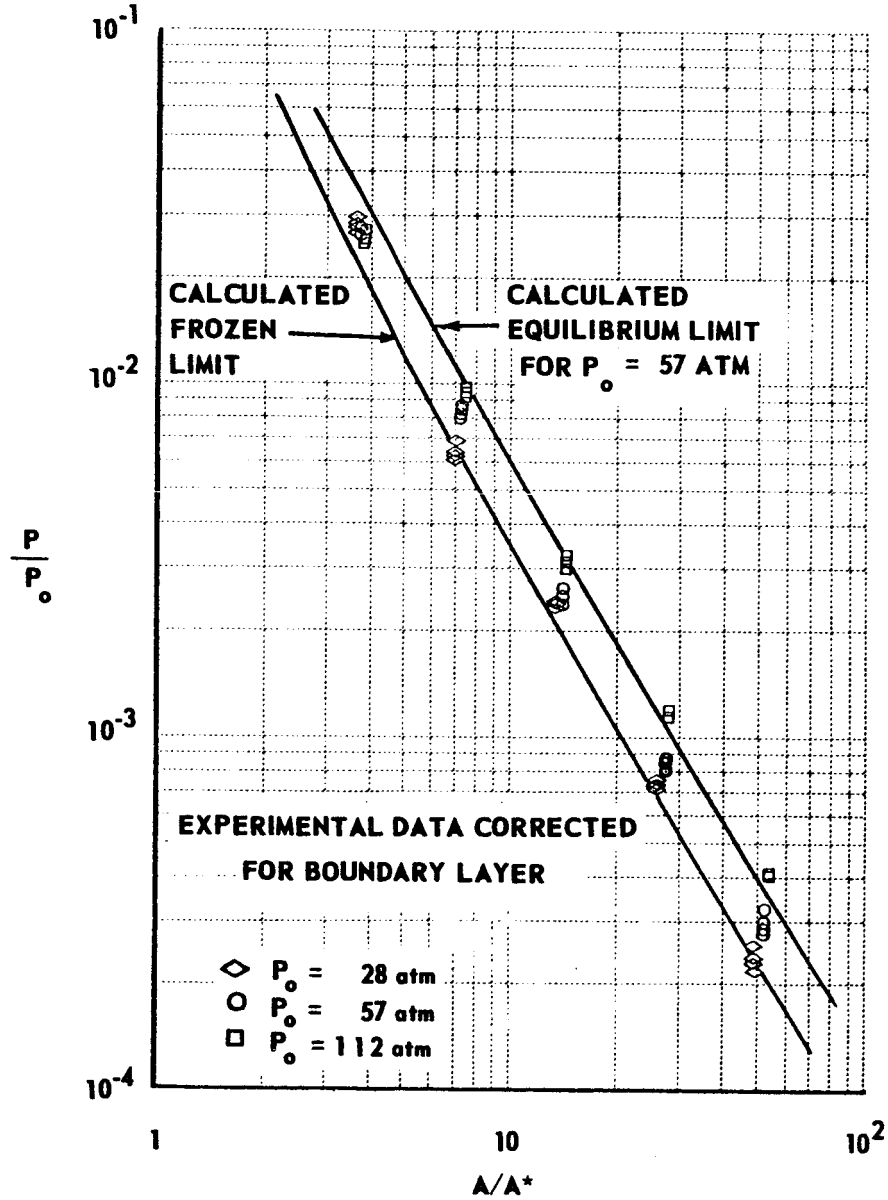

Figure 5 EFFECT OF RESERVOIR PRESSURE P_o ON MEASURED PRESSURE DISTRIBUTIONS FOR FLOW OF DISSOCIATED H_2-Ar MIXTURE IN 15° CONICAL NOZZLE. T_o = 6000°K. UNDISSOCIATED MIXTURE 7.95% H_2 + 92.05% Ar.

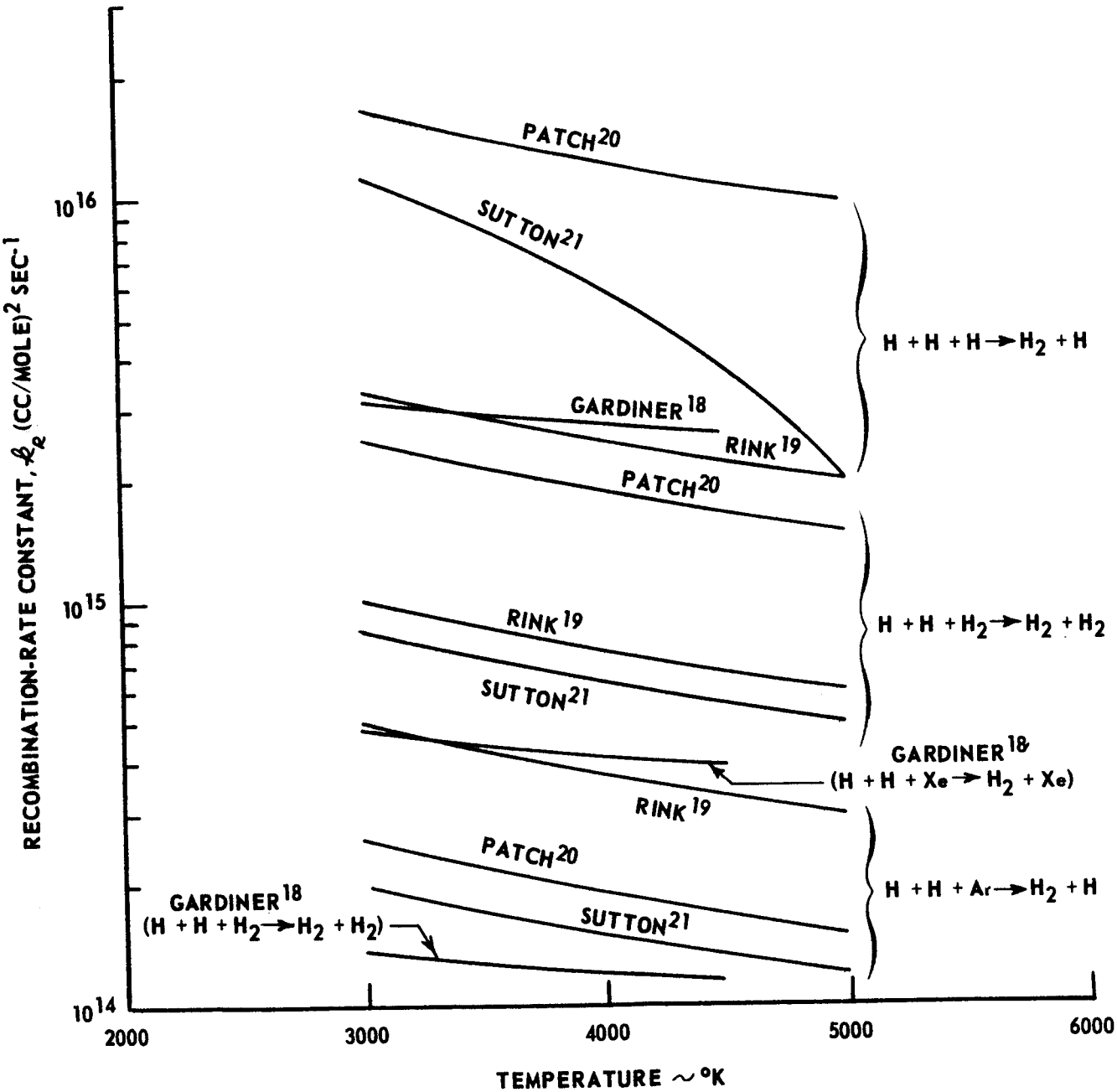

Figure 6 SUMMARY OF HYDROGEN RECOMBINATION RATE CONSTANTS INFERRED FROM SHOCK WAVE DISSOCIATION STUDIES

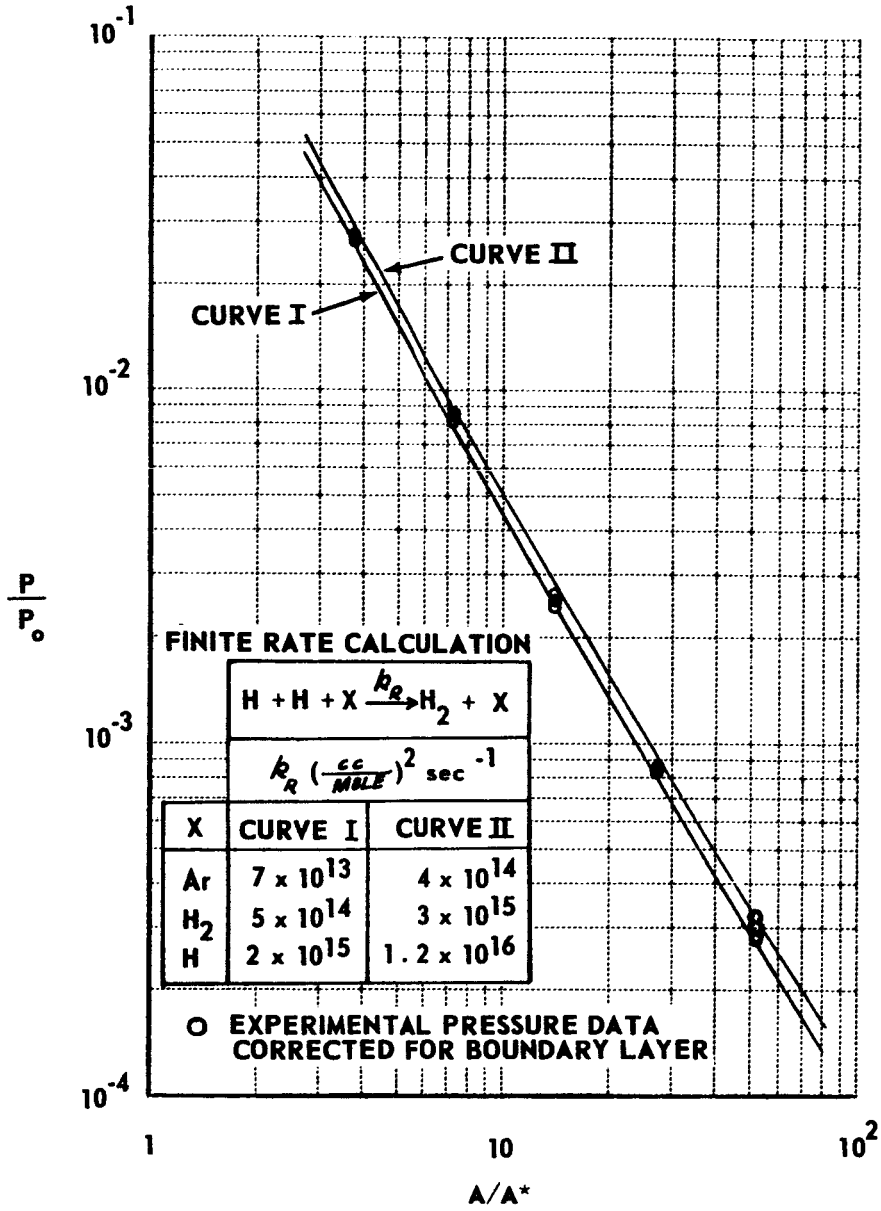

Figure 7 COMPARISON OF MEASURED PRESSURE DISTRIBUTIONS WITH FINITE RATE CALCULATIONS FOR FLOW OF DISSOCIATED H_2 + Ar MIXTURE IN 15° CONICAL NOZZLE. T_o = 6000°K, P_o = 57 ATM UNDISSOCIATED MIXTURE 7.95% H_2 + 92.05% Ar

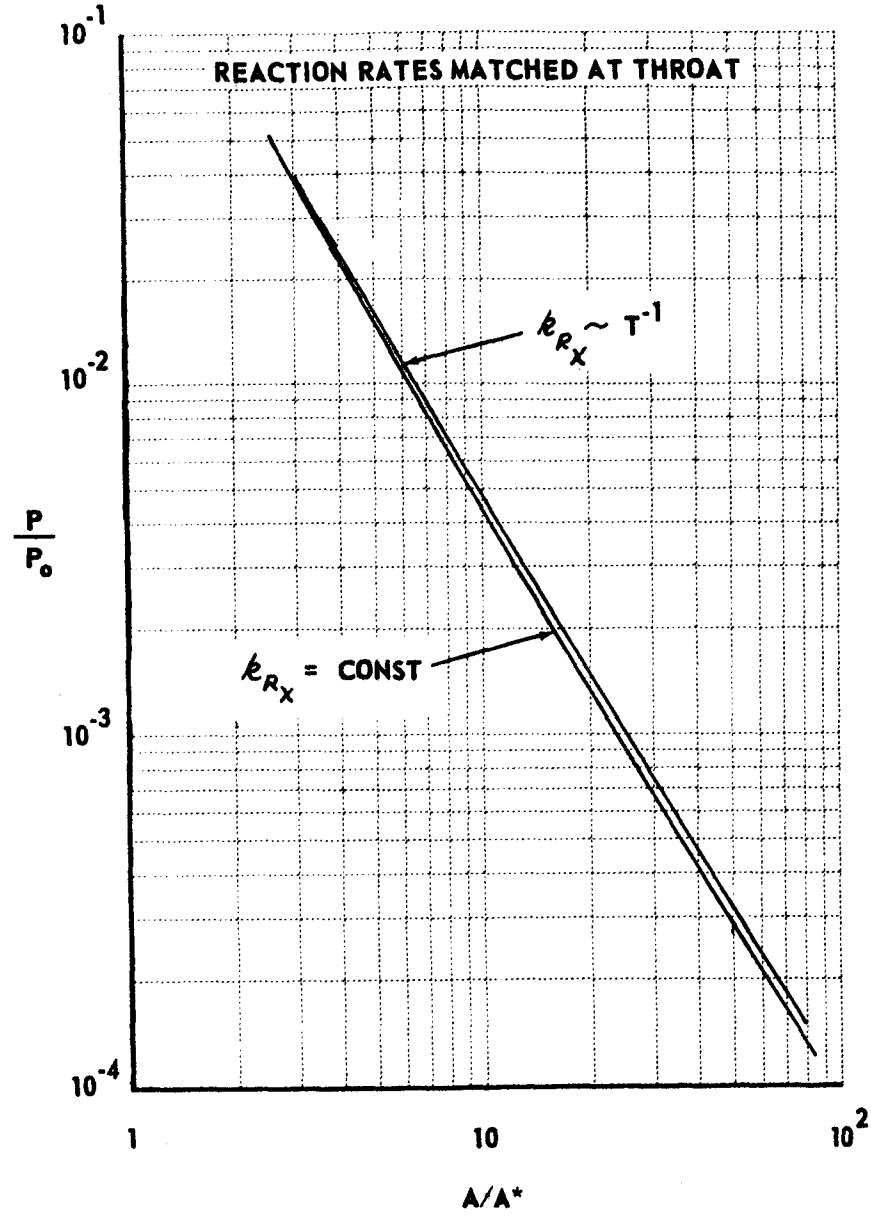

Figure 8 EFFECT OF TEMPERATURE DEPENDENCY OF REACTION RATES ON CALCULATED FINITE RATE FLOW OF DISSOCIATED H_2-Ar MIXTURE IN CONICAL NOZZLE. T_o = 6000°K P_o = 57 ATM UNDISSOCIATED MIXTURE 7.95% H_2 + 92.05% Ar

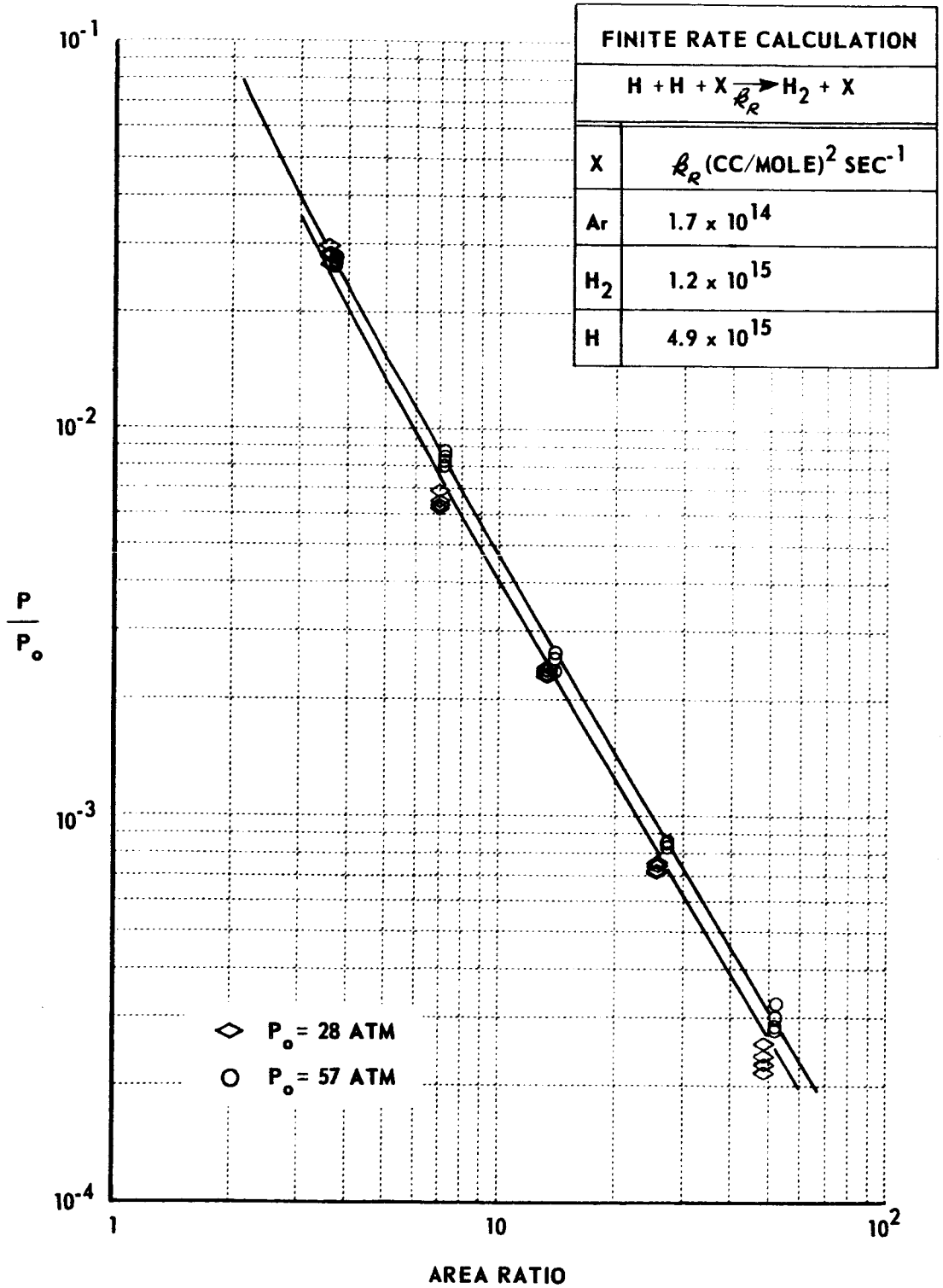

Figure 9 COMPARISON OF CALCULATIONS AND EXPERIMENTAL DATA FOR FLOW OF DISSOCIATED H_2 – Ar MIXTURES IN A 15° CONICAL NOZZLE. T_o = 6000°K, UNDISSOCIATED MIXTURE 7.95% H_2 + 92.05% Ar

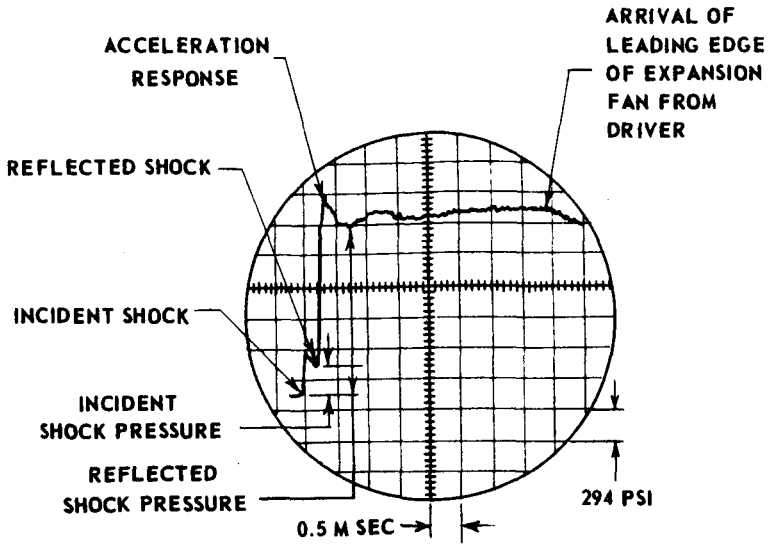

NITROGEN TEST GAS AT 760 MM Hg abs INITIAL PRESSURE
HELIUM DRIVER GAS AT 2000 PSIA INITIAL PRESSURE
MEASURED INCIDENT SHOCK VELOCITY = 4400 fps

NEAR-TAILORED

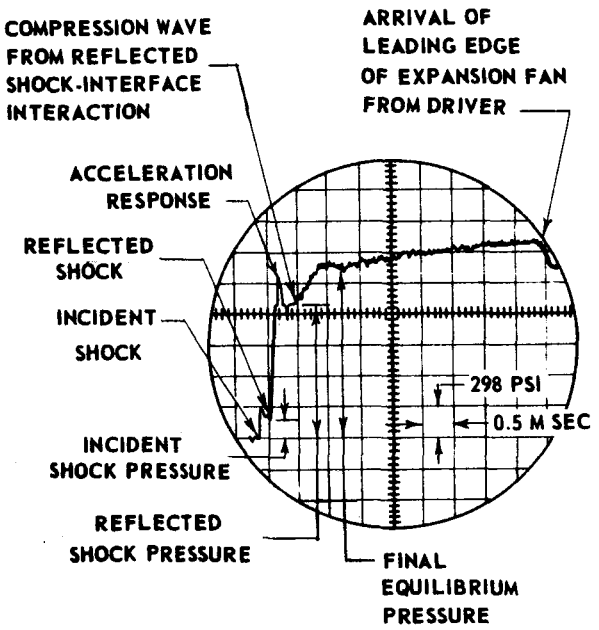

NITROGEN TEST GAS AT 380 MM Hg abs INITIAL PRESSURE
HELIUM DRIVER GAS AT 2140 PSIA INITIAL PRESSURE
MEASURED INCIDENT SHOCK VELOCITY = 5260 fps

UNDER-TAILORED

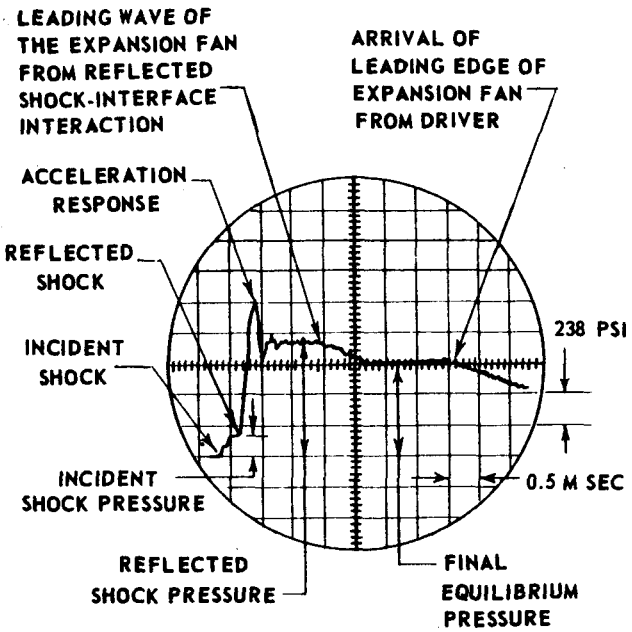

NITROGEN TEST GAS AT 760 MM Hg abs INITIAL PRESSURE
HELIUM DRIVER GAS AT 890 PSIA INITIAL PRESSURE
MEASURED INCIDENT SHOCK VELOCITY = 3860 fps

OVER-TAILORED

Figure 10 TYPICAL PRESSURE RECORDS FOR OFF-TAILORED AND NEAR-TAILORED REFLECTED SHOCK CONDITIONS IN NITROGEN

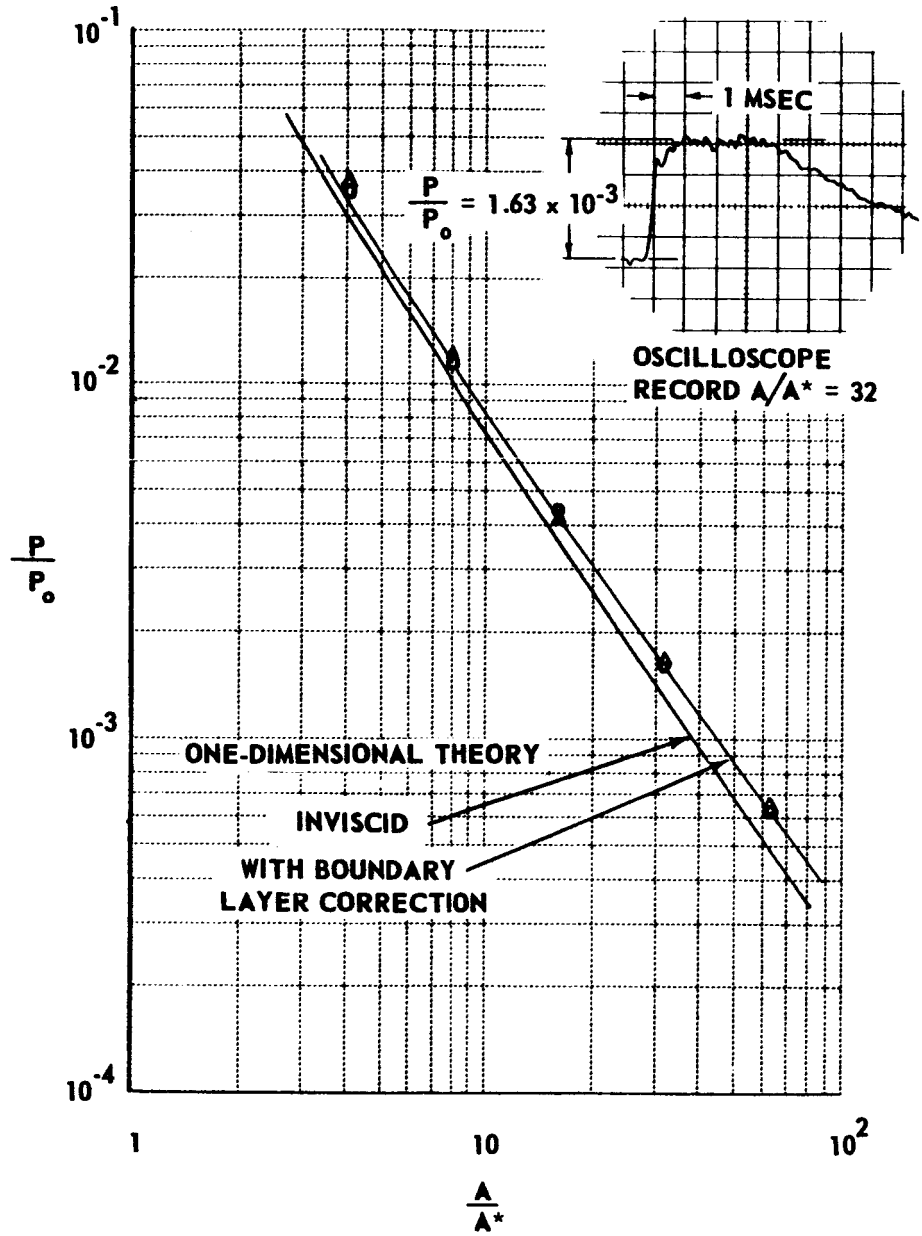

Figure 11 TYPICAL PRESSURE DATA MEASURED IN CALIBRATION EXPERIMENTS TO ASSESS BOUNDARY LAYER EFFECTS IN 15° CONICAL NOZZLE
N_2, T_o = 2000°K, P_o = 60 ATM

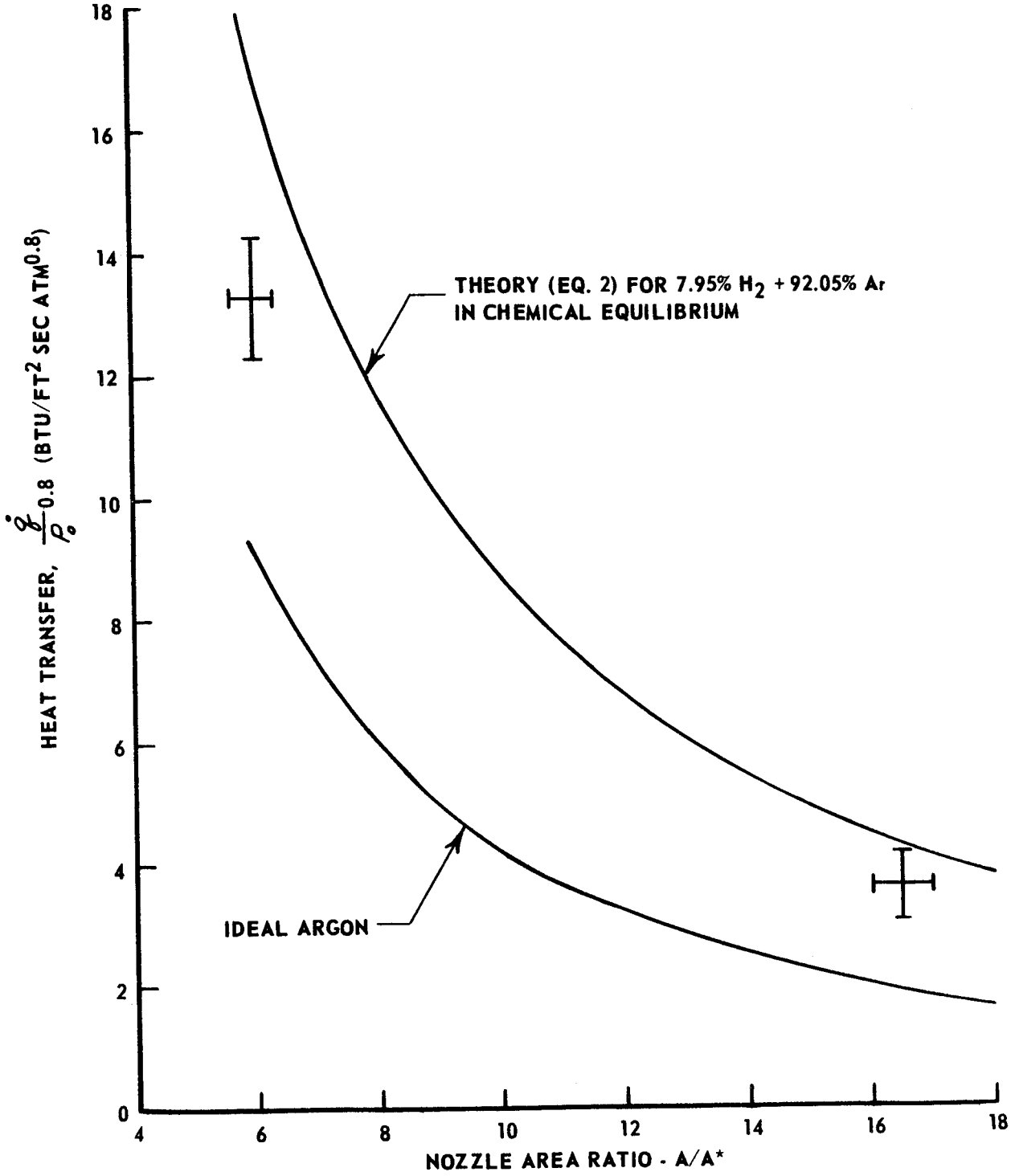

Figure 12 HEAT TRANSFER RATES MEASURED FOR HYDROGEN-ARGON TEST GAS FLOW IN THE WEDGE NOZZLE. ALL DATA NORMALIZED TO RESERVOIR TEMPERATURE OF 5500°K

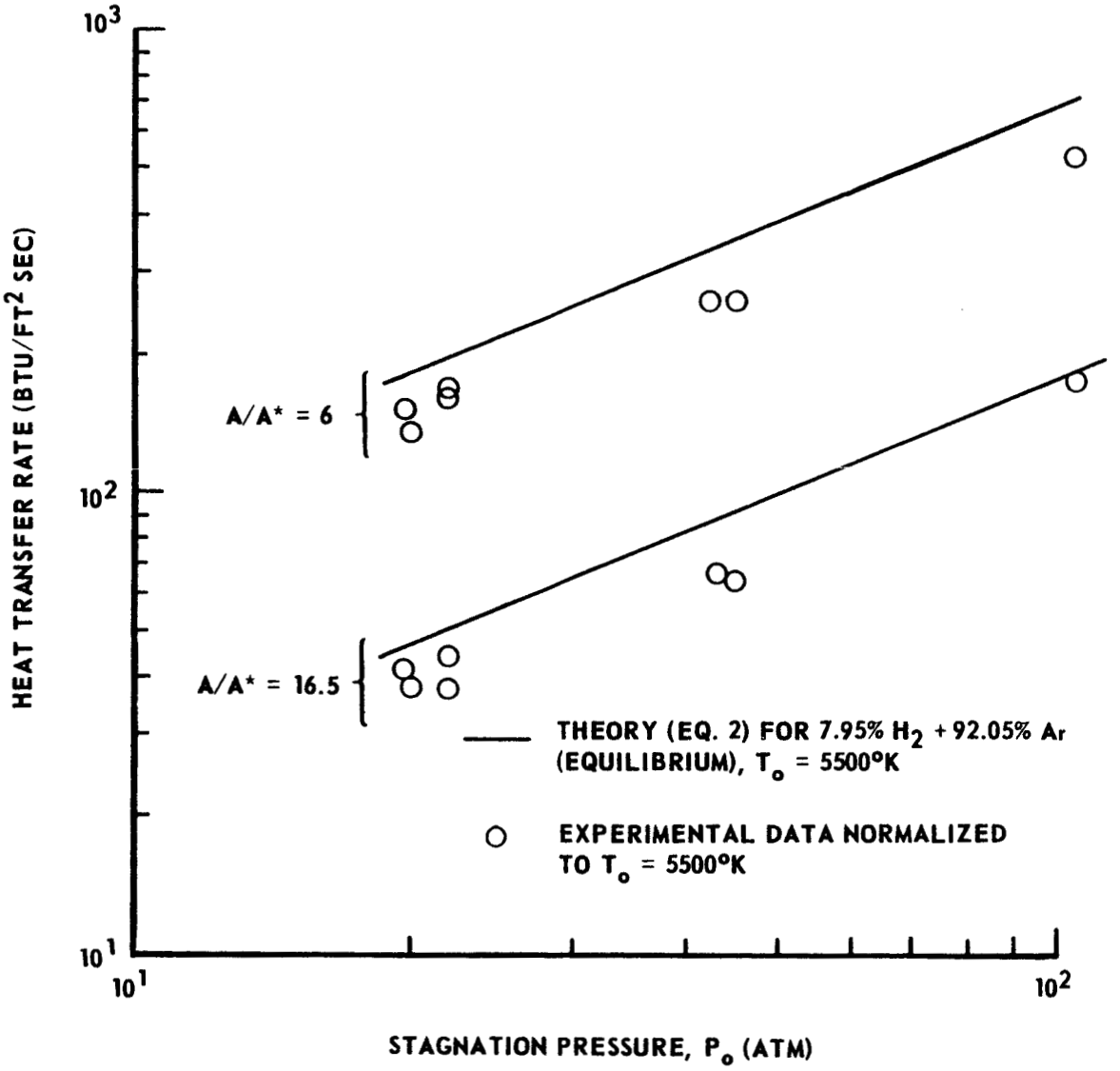

Figure 13 HEAT TRANSFER RATES FOR HYDROGEN-ARGON TEST GAS FLOW IN THE WEDGE NOZZLE